

ADVANCED QUANTUM PHYSICS

Duration : 3 hours

Infrared spectrum of carbon dioxide

In 1896, physicist Svante Arrhenius published an article highlighting the climatic impact of carbon dioxide (CO₂), whose vibrations absorb part of the black body radiation emitted by the Earth. A few years later, however, his theory was challenged by Knut Ångström, who argued that the atmosphere is already completely opaque to the infrared wavelength absorbed by CO₂. A variant of this argument is still used today by climate change deniers. The argument put forward is that the concentration of CO₂ already present in the atmosphere is sufficient to absorb all the radiation emitted by the Earth at the vibration frequency of the molecule, so that a further increase in CO₂ will have no consequence on the climate. While this claim is obviously erroneous, its refutation requires the use of a radiative transfer model of the atmosphere based on precise knowledge of the shape of the infrared absorption spectrum of CO₂. This is the spectrum that will be studied in the following.

The interaction between a CO₂ molecule and the oscillating electric field $\vec{\mathcal{E}}(t) = \vec{\mathcal{E}}_0 \cos \omega t$ associated with an infrared radiation of angular frequency ω can be treated using time-dependent perturbation theory. It is recalled that this interaction can give rise to a transition between an initial state $|i\rangle$ and a final state $|f\rangle$, provided that the frequency ω is very close to the transition frequency $\omega_{fi} = (E_f - E_i)/\hbar$. The transition probability can then be written as

$$\mathcal{P}_{i \rightarrow f} \propto |\langle f | \hat{\vec{\mu}} \cdot \vec{\mathcal{E}}_0 | i \rangle|^2, \quad (1)$$

where $\hat{\vec{\mu}}$ is the electric dipole operator of the molecule.

Exercise 1

CO₂ Vibration modes

CO₂ is a linear triatomic molecule composed of two oxygen atoms (isotope ¹⁶O) located on either side of the central carbon atom (isotope ¹²C), as shown in Fig. 1(a). Since the nuclear spins of the considered isotopes are zero and the molecule is assumed to always be in its electronic ground state, only the motion of the nuclei will be taken into account. The center of mass of the molecule, whose motion is irrelevant for infrared absorption, will be assumed to be stationary and positioned at the origin of the coordinate system. Finally, for this and the following exercise, the molecule will be assumed to be oriented along the z axis.

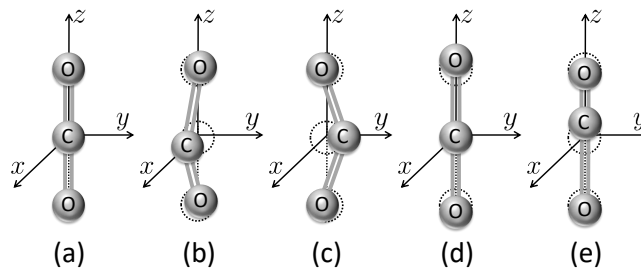


FIGURE 1 – (a) Equilibrium structure of the CO₂ molecule. (b) Bending mode along the x axis, with angular frequency ω_1 . (c) Bending mode along the y axis, with angular frequency ω_1 . (d) Symmetric stretching mode (along the z axis), with angular frequency ω_2 . (e) Antisymmetric stretching mode (along the z axis), with angular frequency ω_3 .

Under these assumptions, the motion of the nuclei can be decomposed into four independent *vibrational modes*, shown in Fig. 1, each described using a harmonic oscillator. First, there are two bending modes : one along the x axis (b) and the other along the y axis (c), both associated with a two-dimensional harmonic oscillator of angular frequency ω_1 . Second, there are two stretching modes, in which the nuclei move along the z axis : the symmetric stretching mode (d), where the carbon nucleus remains stationary while the two oxygen nuclei oscillate symmetrically about the origin. This mode

is described as a one-dimensional harmonic oscillator with angular frequency ω_2 . Finally, there is the antisymmetric stretching mode (e), in which the carbon nucleus moves in the opposite direction to the two oxygen nuclei. This mode is described as a one-dimensional harmonic oscillator with angular frequency ω_3 . The vibrational frequencies are given as $\omega_1/(2\pi) \approx 20.0$ THz, $\omega_2/(2\pi) \approx 40.1$ THz, and $\omega_3/(2\pi) \approx 70.4$ THz, where $1 \text{ THz} = 10^{12} \text{ Hz}$.

1. We consider initially only the antisymmetric stretching mode, with angular frequency ω_3 . The stretching is characterized by the real quantity $\zeta = z_c - (z_1 + z_2)/2$, where z_c is the coordinate of the carbon nucleus, and z_1 and z_2 are the coordinates of the oxygen nuclei. We work within the state space $\mathcal{E}_3 = \mathcal{L}^2(\mathbb{R})$ and introduce the annihilation operator

$$\hat{a}_3 = \frac{1}{\sqrt{2}} \left(\sqrt{\frac{m_r \omega_3}{\hbar}} \hat{\zeta} + i \frac{\hat{p}_\zeta}{\sqrt{m_r \hbar \omega_3}} \right), \quad (2)$$

where $\hat{\zeta}$ and \hat{p}_ζ are the position and momentum observables. The quantity $m_r = 2m_O m_C / (2m_O + m_C)$ is the reduced mass, with m_O and m_C being the masses of the oxygen and carbon nuclei, respectively. The Hamiltonian associated with this vibrational mode can then be written as :

$$\hat{H}_3 = \hbar \omega_3 \left(\hat{a}_3^\dagger \hat{a}_3 + \frac{\hat{I}}{2} \right), \quad (3)$$

where \hat{I} is the identity operator. The eigenstates of \hat{H}_3 will be denoted as $|n\rangle$, with $n \in \mathbb{N}$. Recall the values and degeneracies of the energy levels.

We have $E_n = (n + 1/2)\hbar\omega_3$, where $n \in \mathbb{N}$. For a one-dimensional harmonic oscillator, the energy levels are non-degenerate.

2. Using a numerical application, show that for this mode it is justified to consider that only the ground state $|0\rangle$ is populated at the temperature of the Earth's atmosphere ($T = 288 \text{ K}$).

Let us set $k_B T = \hbar \omega_T$, where ω_T is a frequency characteristic of thermal agitation. We obtain $\omega_T/(2\pi) = k_B T/h \approx 6$ THz, which is very small compared to the transition frequency $\omega_3/(2\pi) \approx 70$ THz. We can therefore deduce that the probability of thermal excitation to the $n = 1$ level will be very low. More precisely, the Boltzmann factor is written as

$$\exp\left(-\frac{E_1 - E_0}{k_B T}\right) = \exp\left(-\frac{\omega_3}{\omega_T}\right) \approx \exp\left(-\frac{70.4}{6}\right) \approx 8 \times 10^{-6} \ll 1.$$

We can therefore consider that only the ground state is populated at the temperature of the Earth's atmosphere.

3. Show that the dipole operator associated with the antisymmetric stretching mode reads

$$\hat{\vec{\mu}} = \mu_3 \left(\hat{a}_3 + \hat{a}_3^\dagger \right) \vec{u}_z, \quad (4)$$

where \vec{u}_z is a unit vector along the z axis. Express the real quantity μ_3 in terms of the problem's parameters and the partial charge δq carried by the carbon atom.

Since the molecule is electrically neutral, we can state that each oxygen atom carries a charge of $-\delta q/2$. We thus have

$$\vec{\mu} = \left(\delta q z_c - \frac{\delta q}{2} z_1 - \frac{\delta q}{2} z_2 \right) \vec{u}_z = \delta q \zeta \vec{u}_z.$$

Furthermore,

$$\hat{a}_3 + \hat{a}_3^\dagger = \sqrt{\frac{2m_r \omega_3}{\hbar}} \hat{\zeta},$$

which yields

$$\hat{\vec{\mu}} = \delta q \sqrt{\frac{\hbar}{2m_r \omega_3}} \left(\hat{a}_3 + \hat{a}_3^\dagger \right) \vec{u}_z.$$

We thus obtain eq. 4, with $\mu_3 = \delta q \sqrt{\hbar/(2m_r \omega_3)}$.

4. Using eq. 1, identify the only transition associated with the antisymmetric stretching mode that can be excited by the infrared field and provide the corresponding transition frequency.

Knowing that only the state $|0\rangle$ is initially populated, let us calculate the matrix element enabling a transition to state $|n\rangle$. We have

$$\langle n | \hat{\vec{\mu}} \cdot \vec{\mathcal{E}}_0 | 0 \rangle = \mu_3 \mathcal{E}_{0z} \langle n | (\hat{a}_3 + \hat{a}_3^\dagger) | 0 \rangle = \mu_3 \mathcal{E}_{0z} \langle n | 1 \rangle.$$

It follows that only state $|1\rangle$ can be excited from state $|0\rangle$, the corresponding transition frequency being $(E_1 - E_0)/\hbar = \omega_3$.

5. We now consider the symmetric stretching mode. What can be said about the dipole observable $\hat{\vec{\mu}}$ in this case?

In the case of the symmetric mode, we have $\hat{z}_1 + \hat{z}_2 = 0$, while $\hat{z}_c = 0$ (since the center of mass is stationary and the carbon atom remains stationary at the origin). We deduce that the dipole observable is zero.

6. Comment Fig. 2, which represents the infrared absorption spectrum of CO_2 . Among the 4 vibration modes considered above, which are relevant in the context of the climate impact of CO_2 ?

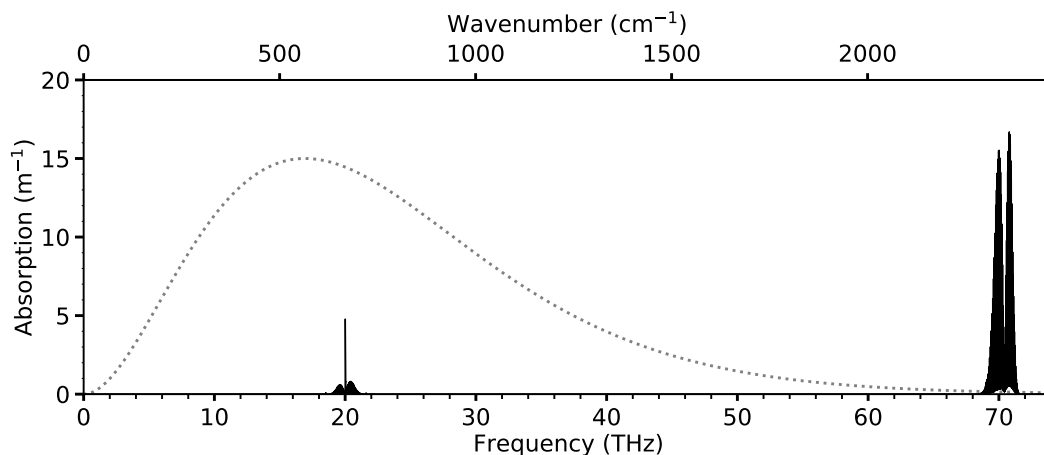


FIGURE 2 – Absorption spectrum of CO_2 in the mid-infrared range, for a CO_2 concentration of 426 ppm in air at atmospheric pressure and at a temperature of $T = 288$ K. The dashed line represents, in arbitrary units, the black body emission spectrum for $T = 288$ K.

A strong infrared absorption is observed at frequency $\omega_3/(2\pi) \approx 70$ THz, which can thus be attributed to the antisymmetric stretching mode. Absorption is also observed at frequency $\omega_1/(2\pi) \approx 20$ THz, which can be attributed to the bending motion associated with a dipole oscillating in the xy plane, induced by the components of the infrared field oscillating in this plane. As expected, no absorption is observed at the frequency of the symmetric stretching mode $\omega_2/(2\pi) \approx 40$ THz. Indeed, since the dipole is zero, the transition probability is also zero, and this vibration mode is therefore not coupled to infrared radiation. As the mode with frequency ω_3 is beyond the Earth's black body emission spectrum, we can conclude that only the two bending modes, with angular frequency ω_1 , will have an impact on the climate.

7. It can be read from Fig. 2 that absorption α at angular frequency ω_1 is approximately 4.8 m^{-1} . Knowing that the resulting transmission after propagation over a distance L is given by $\exp(-\alpha L)$, deduce the value of L required for the photon transmission probability to be less than 10^{-6} . Comment on this result.

The required length must be greater than $-\ln(10^{-6})/4.8 \approx 2.9$ m. This distance being much smaller than the thickness of the atmosphere, we can conclude that the atmosphere is indeed already opaque at this frequency. *However, it is important to consider the entire spectrum to draw conclusions about the climate effect of an increase in CO_2 concentration.*

Exercice 2 Fermi Resonance

This exercise deals with the bending motion shown in Fig. 1(b) and (c).

1. Two-dimensional harmonic oscillator

Given the small value of the bending angle, we can assume that the nuclei move within horizontal planes. Let (x, y) represent the coordinates of the carbon nucleus relative to the projection of the two oxygen nuclei in the xy -plane. We introduce the observables \hat{x} and \hat{y} associated with these coordinates, as well as the corresponding momentum observables \hat{p}_x and \hat{p}_y . Operator \hat{a}_x (respectively \hat{a}_y) can then be constructed using an equation similar to eq. 2, by replacing ω_3 with ω_1 , and substituting $\hat{\zeta}$ and \hat{p}_ζ with \hat{x} and \hat{p}_x (respectively \hat{y} and \hat{p}_y). We work in the state space $\mathcal{E}_1 = \mathcal{L}^2(\mathbb{R}^2) = \mathcal{L}^2(\mathbb{R}) \otimes \mathcal{L}^2(\mathbb{R})$, and the Hamiltonian of the system is expressed as $\hat{H}_1 = \hat{H}_x + \hat{H}_y$, where $\hat{H}_x = \hbar\omega_1 \left(\hat{a}_x^\dagger \hat{a}_x + \hat{I}/2 \right)$ and $\hat{H}_y = \hbar\omega_1 \left(\hat{a}_y^\dagger \hat{a}_y + \hat{I}/2 \right)$.

1.1 Explain why \hat{H}_x and \hat{H}_y can be co-diagonalized, and show that the eigenvalues of \hat{H}_1 are $E_n = (n+1)\hbar\omega_1$, with $n \in \mathbb{N}$. Specify the associated degeneracies.

\hat{H}_x and \hat{H}_y act in two different spaces and therefore commute with each other. The tensorial basis $\{|n_x\rangle \otimes |n_y\rangle\}$, constructed from the eigenstates of the one-dimensional harmonic oscillator, is thus a common eigenbasis of these two operators, and therefore of \hat{H}_1 . We have :

$$\hat{H}_1 |n_x\rangle \otimes |n_y\rangle = (n_x + 1/2 + n_y + 1/2)\hbar\omega_1 |n_x\rangle \otimes |n_y\rangle,$$

where n_x and n_y are integers. We thus obtain the announced result, with $n = n_x + n_y$. For a given value of n , we have $n_x \in \{0, 1, \dots, n\}$ and $n_y = n - n_x$, which gives us $n+1$ independent states. The degeneracy of E_n is therefore equal to $n+1$.

1.2 Let us introduce operators $\hat{a}_\pm = (\hat{a}_x \mp i\hat{a}_y)/\sqrt{2}$, which commute with each other and, along with their adjoints, satisfy the usual commutation relations of annihilation and creation operators associated with a one-dimensional harmonic oscillator. Show that $\hat{H}_1 = \hbar\omega_1 \left(\hat{N}_+ + \hat{N}_- + \hat{I} \right)$, where $\hat{N}_\pm = \hat{a}_\pm^\dagger \hat{a}_\pm$. Recover with this alternative method the eigenvalues of \hat{H}_1 and their degeneracies. We have

$$\hat{N}_\pm = \frac{1}{2}(\hat{a}_x^\dagger \pm i\hat{a}_y^\dagger)(\hat{a}_x \mp i\hat{a}_y) = \frac{1}{2} \left(\hat{a}_x^\dagger \hat{a}_x + \hat{a}_y^\dagger \hat{a}_y \right) \pm \frac{i}{2} \left(\hat{a}_y^\dagger \hat{a}_x - \hat{a}_x^\dagger \hat{a}_y \right).$$

It follows that $\hat{N}_+ + \hat{N}_- = \hat{a}_x^\dagger \hat{a}_x + \hat{a}_y^\dagger \hat{a}_y$, which allows us to establish the expression for \hat{H}_1 as announced. We then deduce that the eigenvalues are of the form $(n+1)\hbar\omega_1$, where $n = n_+ + n_-$, which confirms the announced degeneracy since $n_+ \in \{0, 1, \dots, n\}$ and $n_- = n - n_+$.

1.3 We note $\hat{K} = \hbar(\hat{N}_+ - \hat{N}_-)$ the projection of the angular momentum along the z -axis of the molecule. Explain the physical reason why \hat{K} commutes with \hat{H}_1 .

Since the system is invariant under rotation around the z -axis, we have $[\hat{K}, \hat{H}_1] = 0$.

1.4 We consider the common eigenbasis of the ECO $\{\hat{H}_1, \hat{K}\}$ for the eigenvalues $(n+1)\hbar\omega_1$ and $k\hbar$, which will simply be denoted as $|n, k\rangle$ throughout the rest of this text. Show that $|n, k\rangle$ is an eigenvector of \hat{N}_+ and \hat{N}_- for the eigenvalues n_+ and n_- , which will be expressed in terms of n and k .

We have $(\hat{N}_+ + \hat{N}_-) |n, k\rangle = n |n, k\rangle$ and $(\hat{N}_+ - \hat{N}_-) |n, k\rangle = k |n, k\rangle$. By taking linear combinations of these expressions, we obtain

$$\begin{aligned} \hat{N}_+ |n, k\rangle &= \frac{n+k}{2} |n, k\rangle, \\ \hat{N}_- |n, k\rangle &= \frac{n-k}{2} |n, k\rangle, \end{aligned}$$

which establishes the desired result with $n_\pm = \frac{n \pm k}{2}$.

1.5 Show that k is an integer with the same parity as n and belonging to the interval $[-n, n]$.

It follows that $k = n_+ - n_- = 2n_+ - n$. Since n_+ is an integer between 0 and n , it follows that k is an integer between $-n$ and n , with the same parity as n because $n+k = 2n_+$ is even.

1.6 Show that $\hat{a}_\pm |n, k\rangle \propto |n-1, k \mp 1\rangle$ and $\hat{a}_\pm^\dagger |n, k\rangle \propto |n+1, k \pm 1\rangle$.

We know that $|n, k\rangle$ is an eigenvector of the observables \hat{N}_\pm with eigenvalues $n_\pm = (n \pm k)/2$. Therefore, $\hat{a}_+ |n, k\rangle$ is an eigenvector of \hat{N}_+ and \hat{N}_- with eigenvalues $n_+ - 1$ and n_- , which means that $n = n_+ + n_-$ decreases by 1, as does $k = n_+ - n_-$. Thus, $\hat{a}_+ |n, k\rangle$ is an eigenvector of $\hat{N} = \hat{N}_+ + \hat{N}_-$ and \hat{K} with eigenvalues $n-1$ and $k-1$, respectively. It is therefore proportional to $|n-1, k-1\rangle$. We can apply the same reasoning for the action of \hat{a}_- , which swaps the roles of n_+ and n_- . The number $n = n_+ + n_-$ still decreases by one unit, while k increases by 1.

Hence, we obtain a vector proportional to $|n-1, k+1\rangle$. Regarding the action of \hat{a}_\pm^\dagger , the number n_\pm is incremented, which increments n and adds ± 1 to $k = n_+ - n_-$. We thus obtain the desired relations.

We could also write $|n, k\rangle = |n_+ = (n+k)/2, n_- = (n-k)/2\rangle$ and then

$$\begin{aligned}\hat{a}_+ |n, k\rangle &= \hat{a}_\pm |n_+ = \frac{n+k}{2}, n_- = \frac{n-k}{2}\rangle \\ &= \sqrt{\frac{n+k}{2}} |n_+ = \frac{n+k}{2} - 1, n_- = \frac{n-k}{2}\rangle \\ &= \sqrt{\frac{n+k}{2}} |n-1, k-1\rangle,\end{aligned}$$

and so on.

1.7 In the rest of this exercise, we assume that the infrared field is polarized along the x axis. We consider the Cartesian component along this axis of the dipole operator, $\hat{\mu}_x = \delta q \hat{x}$. Express $\hat{\mu}_x$ in terms of the operators \hat{a}_\pm and their adjoints, and then show that if the system is initially in the state $|n, k\rangle$, the infrared field can induce a transition to final state $|n', k'\rangle$ only if $n' = n \pm 1$ and $k' = k \pm 1$.

We will say that the transition follows the selection rule $\Delta n = \pm 1$ and $\Delta k = \pm 1$.

We have

$$\hat{a}_x + \hat{a}_x^\dagger = \sqrt{\frac{2m_r\omega_1}{\hbar}} \hat{x}$$

or $\hat{a}_x = (\hat{a}_+ + \hat{a}_-)/\sqrt{2}$. From this, we deduce

$$\hat{\mu}_x = \delta q \sqrt{\frac{\hbar}{4m_r\omega_1}} (\hat{a}_+ + \hat{a}_- + \hat{a}_+^\dagger + \hat{a}_-^\dagger)$$

Using the result from the previous question, we deduce that the matrix element $\langle n', k' | \hat{\mu}_x | n, k \rangle$ can only be non-zero if $n' = n \pm 1$ and $k' = k \pm 1$, which establishes the announced selection rule.

2. Anharmonic coupling between vibrational modes

We are interested in the anharmonic coupling between the bending modes and the symmetric stretching mode, a coupling that is exacerbated by what is called a *Fermi resonance*. This results from the near-equality between $2\omega_1/(2\pi) = 40.0$ THz and $\omega_2/(2\pi) = 40.1$ THz. For simplicity, we will replace ω_2 by $2\omega_1$ in this part. Moreover, the antisymmetric stretching mode will not be considered, which amounts to working in the space $\mathcal{E}_1 \otimes \mathcal{E}_2 = \mathcal{L}^2(\mathbb{R}^2) \otimes \mathcal{L}^2(\mathbb{R})$. We will use the tensorial basis $\{|n_1, k; n_2\rangle = |n_1, k\rangle \otimes |n_2\rangle\}$, where $\{|n_1, k\rangle\}$ is the common eigenbasis of \hat{H}_1 and \hat{K} introduced in the previous part (with $k \in \{-n_1, -n_1+2, \dots, n_1\}$), and where $\{|n_2\rangle\}$ is the eigenbasis of the Hamiltonian \hat{H}_2 of the harmonic oscillator with frequency $\omega_2 = 2\omega_1$ associated with the symmetric stretching mode. The anharmonic coupling will be taken into account with an additional term \hat{W} to be added to the unperturbed Hamiltonian $\hat{H}_1 + \hat{H}_2$. The effect of \hat{W} will be treated at first order in time-independent perturbation theory. By symmetry, we will assume that all diagonal terms of the form $\langle n_1, k; n_2 | \hat{W} | n_1, k; n_2 \rangle$ are zero.

2.1 Write the action of $\hat{H}_1 + \hat{H}_2$ on $|n_1, k; n_2\rangle$, then express the energy of the first three levels in terms of $\hbar\omega_1$ (in the absence of perturbation). For each level, provide the vectors of the tensorial basis that generate the corresponding eigenspace.

We have

$$(\hat{H}_1 + \hat{H}_2) |n_1, k; n_2\rangle = ((n_1 + 1)\hbar\omega_1 + (n_2 + 1/2)\hbar\omega_2) |n_1, k; n_2\rangle = (n_1 + 2n_2 + 2)\hbar\omega_1 |n_1, k; n_2\rangle.$$

The ground state thus has energy $E_0 = 2\hbar\omega_1$. It is non-degenerate and the corresponding eigenvector is $|0, 0; 0\rangle$. The first excited state has energy $E_0 + \hbar\omega_1$. It is doubly degenerate and has the eigenbasis $\{|1, -1; 0\rangle, |1, 1; 0\rangle\}$. The second excited state has energy $E_0 + 2\hbar\omega_1$. It is fourfold degenerate and has the eigenbasis $\{|2, -2; 0\rangle, |2, 2; 0\rangle, |2, 0; 0\rangle, |0, 0; 1\rangle\}$.

2.2 By proceeding as in question 2 of exercise 1, show that the probability of finding the system in the first excited state is not completely negligible.

Since the energy difference between the first excited state and the ground state is $\hbar\omega_1$, the Boltzmann factor now reads

$$\exp\left(-\frac{\omega_1}{\omega_T}\right) \approx \exp\left(-\frac{20}{6}\right) \approx 3.6 \times 10^{-2},$$

which is no longer negligible.

2.3 Explain why operator \hat{K} commutes with \hat{W} .

The observable \hat{K} corresponds to the total angular momentum of the system (since there is no contribution to the angular momentum from the stretching mode, whose state is obviously unchanged by rotation). Due to the rotational invariance of the system, it can be deduced that \hat{K} commutes with \hat{W} .

2.4 Calculate $\langle n_1, k; n_2 | [\hat{W}, \hat{K}] | n'_1, k'; n'_2 \rangle$ in two different ways, and then deduce that the matrix elements $\langle n_1, k; n_2 | \hat{W} | n'_1, k'; n'_2 \rangle$ are zero whenever $k \neq k'$.

We have

$$\begin{aligned} \langle n_1, k; n_2 | [\hat{W}, \hat{K}] | n'_1, k'; n'_2 \rangle &= \langle n_1, k; n_2 | (\hat{W}k' - k\hat{W}) | n'_1, k'; n'_2 \rangle \\ &= (k - k') \langle n_1, k; n_2 | \hat{W} | n'_1, k'; n'_2 \rangle. \end{aligned}$$

Moreover, the quantity above is obviously zero since $[\hat{W}, \hat{K}] = 0$. We then deduce that the matrix element of \hat{W} is zero whenever $k \neq k'$.

2.5 Show that \hat{W} has no effect on the first two energy levels (as first order).

The ground state is non-degenerate. The shift in energy to first order is therefore simply equal to $\langle 0, 0; 0 | \hat{W} | 0, 0; 0 \rangle$, which is zero by hypothesis.

The first excited state is doubly degenerate. We must therefore diagonalize the restriction of \hat{W} to the space spanned by $|1, 1; 0\rangle$ and $|1, -1; 0\rangle$. The diagonal matrix elements are zero by hypothesis, while the off-diagonal matrix elements $\langle 1, 1; 0 | \hat{W} | 1, -1; 0 \rangle$ are zero according to the result from the previous question. Therefore, the restriction of \hat{W} is zero, and the perturbation has no effect on this level.

2.6 We now consider the effect of \hat{W} on the third energy level, still to first order in perturbation theory. By appropriately ordering the basis vectors, show that the matrix to be considered is block-diagonal, then determine the new position of the energy levels as well as the corresponding eigenbasis. We will denote $\hbar\Omega = \langle 2, 0; 0 | \hat{W} | 0, 0; 1 \rangle$, a quantity which will be assumed to be real.

According to question 2.4, the only non-zero matrix elements of the restriction of \hat{W} are those connecting states with the same value of k . Therefore, the states corresponding to $k = \pm 2$ are not coupled to the others. We deduce that the matrix of the restriction of \hat{W} in the basis $\{|2, -2; 0\rangle, |2, 2; 0\rangle, |2, 0; 0\rangle, |0, 0; 1\rangle\}$ is given by

$$\hat{W} = \begin{pmatrix} 0 & 0 & 0 & 0 \\ 0 & 0 & 0 & 0 \\ 0 & 0 & 0 & \hbar\Omega \\ 0 & 0 & \hbar\Omega & 0 \end{pmatrix}.$$

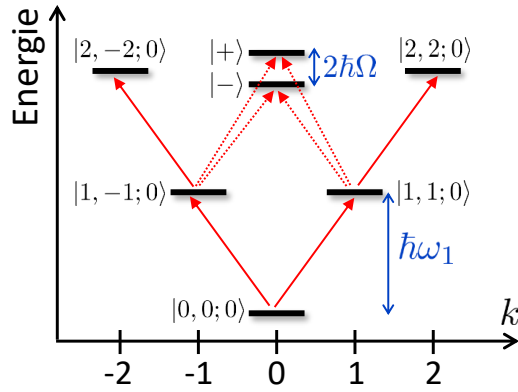
This is indeed a block-diagonal matrix. The first two states, $|2, \pm 2; 0\rangle$, are therefore unaffected by the perturbation, with a total energy remaining equal to $E_0 + 2\hbar\omega_1$. The diagonalization of the remaining 2×2 matrix gives the two states

$$|\pm\rangle = \frac{|2, 0; 0\rangle \pm |0, 0; 1\rangle}{\sqrt{2}},$$

with a total energy of $E_0 + 2\hbar\omega_1 \pm \hbar\Omega$.

2.7 Represent on a diagram the position of the states discussed in 2.5 and 2.6, taking into account the effect of the perturbation \hat{W} . For each state, the horizontal position of the level will correspond to the value of k , while the vertical position of the level will correspond to its energy. Using the selection rules established in 1.7, represent with arrows the transitions allowed under the action of the infrared field.

We obtain the diagram shown below. According to what we have seen in 1.7, the allowed infrared transitions correspond to $\Delta n = \pm 1$ and $\Delta k = \pm 1$.



2.8 The absorption spectrum of CO_2 near the frequency ω_1 is shown in Fig. 3. Here, we focus only on the main lines indicated by vertical dashed lines (the interpretation of the much narrower lines appearing on either side of these main lines will be addressed in the next exercise). Using the energy level diagram constructed in the previous question, interpret the physical origin of the lines observed at 20, 18.5, and 21.6 THz. Does the order of magnitude of the amplitude of the latter two lines seem consistent with the theoretical model?

The two new transitions at $\omega_1 \pm \Omega$ (shown as dashed lines in the above diagram) explain the absorption lines located symmetrically on either side of the transition at ω_1 . We verify that the frequency differences $20.01 - 18.52 = 1.49$ THz and $21.6 - 20.01 = 1.59$ THz are nearly identical, consistent with the expected frequencies at $\omega_1 \pm \Omega$. From this, we deduce $\Omega/(2\pi) \approx 1.55$ THz.

Regarding the amplitude of the lines, the graph shows an attenuation factor of 0.020 (resp. 0.017) for the left (resp. right) line. Theoretically, according to question 2.2, the Boltzmann factor is $\exp(-20/6) \approx 0.036$. Within a factor of 2, this agrees well with the attenuation of the lateral lines by about two orders of magnitude.

To be more thorough, the line amplitude must be multiplied by 2 because there are twice as many initial states available ($k = \pm 1$), then divided by 2 because there are half as many final states available (only $k = 0$ instead of $k = \pm 1$). It must then be multiplied by 2 because the matrix elements of the harmonic oscillator scale with \sqrt{n} , and finally divided by 2 because the final state is mixed with the symmetric stretching mode that does not couple to the light. Ultimately, these four factors of 2 cancel each other out.

2.9 Propose a hypothesis to qualitatively explain the physical origin of the lines observed at 16.3 and 23.7 THz.

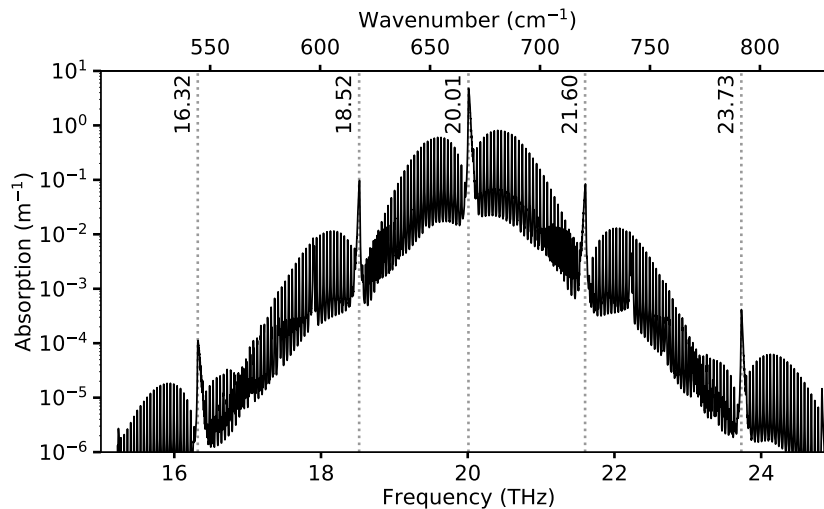
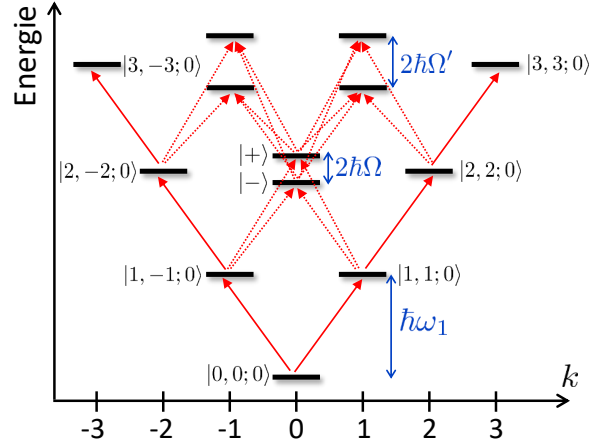


FIGURE 3 – Semi-logarithmic plot of the absorption spectrum of CO_2 in the vicinity of frequency ω_1 .

Similarly, the energy level $E_0 + 3\hbar\omega_1$ (initially sixfold degenerate) will also split, as shown below, with $\hbar\Omega' = \langle 3, 1; 0 | \hat{W} | 1, 1; 1 \rangle$. Additional lines with frequencies $\omega_1 \pm \Omega'$, $\omega_1 \pm (\Omega' - \Omega)$, and $\omega_1 \pm (\Omega' + \Omega)$ are expected. Given the Boltzmann factor, now equal to $\exp(-40/6) \approx 10^{-3}$, these lines will be even less intense. It is expected that only the farthest lines, at frequencies $\omega_1 \pm (\Omega' + \Omega)$, will be visible (at 16.32 and 23.73 THz), while the other four lines will be buried in the rotational background. The measured values for $(\Omega + \Omega')/(2\pi)$ are nearly identical on either side, at 3.69 and

3.72 THz, leading to $\Omega'/\Omega \approx 1.4$.



Knowing this value of Ω' , the lines at $\omega_1 \pm \Omega'$ can be identified at 17.8 and 22.2 THz, slightly emerging from the rotational background.

Exercice 3 Ro-vibrational spectrum of CO₂

The purpose of this exercise is to take into account the rotational motion of the CO₂ molecule, in order to achieve a complete description of its infrared spectrum.

1. Rigid rotor model

We first consider the rigid rotor model, which disregards the vibrations of the molecule. The only remaining degrees of freedom are then associated with the orientation of the molecule in space, described using spherical coordinates θ and φ as shown in Fig. 4. The axis of the molecule is thus represented by the unit vector \vec{u} , defined by the usual expression :

$$\vec{u} = \begin{pmatrix} \sin \theta \cos \varphi \\ \sin \theta \sin \varphi \\ \cos \theta \end{pmatrix} \quad (5)$$

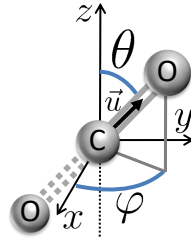


FIGURE 4 – Representation of the CO₂ molecule, assumed to be a rigid rotor whose orientation is determined by the colatitude $\theta \in [0, \pi]$ and the longitude $\varphi \in [0, 2\pi[$.

We consider the Hilbert space \mathcal{E}_{rot} , where the state of the system is entirely determined by a ket $|Y\rangle \in \mathcal{E}_{\text{rot}}$ associated with the angular wavefunction $Y(\theta, \varphi)$. The inner product reads

$$\langle Y_1 | Y_2 \rangle = \int_0^\pi \int_0^{2\pi} Y_1^*(\theta, \varphi) Y_2(\theta, \varphi) \sin \theta \, d\theta d\varphi. \quad (6)$$

The Hamiltonian associated with the rotational motion of the molecule is written as

$$\hat{H}_{\text{rot}} = \frac{\hat{L}^2}{2I} = \hbar B \frac{\hat{L}^2}{\hbar^2}, \quad (7)$$

where \hat{L} is the angular momentum operator and I is the moment of inertia of the molecule. The quantity $B = \hbar/(2I)$ is called the rotational constant of the molecule.

1.1 In the following, we will use the eigenbasis $\{|l, m\rangle\}$ of \hat{L}^2 and \hat{L}_z , consisting of the spherical harmonics $Y_{\ell, m}(\theta, \varphi)$, with $\ell \in \mathbb{N}$. Recall the eigenvalues of \hat{L}^2 as well as the possible values of m .

We have $\hat{L}^2 |l, m\rangle = \ell(\ell + 1)\hbar^2 |l, m\rangle$, where ℓ is an integer. The possible values of m are the $2\ell + 1$ integers between $-\ell$ and $+\ell$.

1.2 Using the rotational constant B , express the energy values E_ℓ of the system, and the associated degeneracies.

We have

$$E_\ell = \ell(\ell + 1)\hbar B,$$

with ℓ integer. The degeneracy of each level is equal to $2\ell + 1$.

1.3 Show in two different ways that the oxygen nuclei considered here are bosons.

The oxygen 16 nucleus contains 16 fermions, which is an even number. It is therefore a boson.

1.4 Exchanging the two nuclei is equivalent to performing a central symmetry with respect to the origin, which is described by the parity operator $\hat{\Pi}$. Knowing that $\hat{\Pi}|\ell, m\rangle = (-1)^\ell |\ell, m\rangle$, what can we deduce about the allowed values of ℓ when taking into account the indistinguishable nature of the oxygen nuclei?

According to the symmetrization postulate, we must restrict ourselves to state vectors unchanged by the exchange of the two nuclei, i.e. states for which ℓ is even.

1.5 In the context of the rigid rotor model, do you think the CO_2 molecule can absorb electromagnetic radiation?

If we note r_0 the length of the CO bond, we can write the dipole operator according to the expression $\hat{\mu} = \delta q \times 0 - (\delta q/2)r_0\hat{u} + (\delta q/2)r_0\hat{u} = 0$. The symmetry of the problem means that the dipole operator is zero. According to eq. 1, the probability of absorption is therefore zero.

2. Ro-vibrational spectrum associated with the antisymmetric stretching mode

We now combine rotational and vibrational motions. For sake of simplicity, we will consider just one mode of vibration, namely the antisymmetric stretching mode with frequency ω_3 . We are therefore in the state space $\mathcal{E}_3 \otimes \mathcal{E}_{\text{rot}}$, where $\mathcal{E}_3 = \mathcal{L}^2(\mathbb{R})$. The vibrational mode considered is that shown in Fig. 1(e), except that the molecule is now aligned according to the vector \vec{u} introduced above. Consequently, eq. 4 expressing the dipole operator must be replaced by

$$\hat{\mu} = \mu_3(\hat{a}_3 + \hat{a}_3^\dagger)\hat{u}, \quad (8)$$

where \hat{a}_3 acts in \mathcal{E}_3 while \hat{u} is now an observable acting in \mathcal{E}_{rot} . The Hamiltonian of the system is written $\hat{H} = \hat{H}_3 + \hat{H}_{\text{rot}}$, where \hat{H}_3 is defined by eq. 3 and \hat{H}_{rot} is defined by eq. 7.

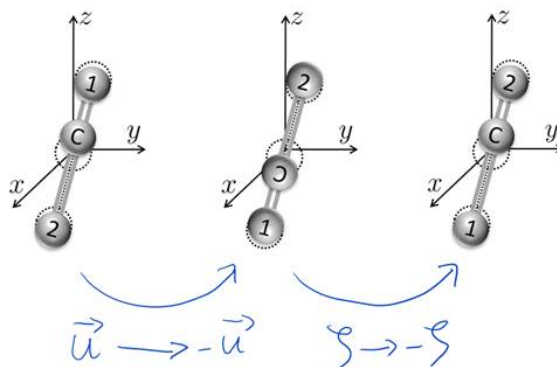
2.1 Write the energy value $E_{n,\ell}$ associated with eigenstate $|n\rangle \otimes |\ell, m\rangle$.

We have

$$E_{n,\ell} = (n + 1/2)\hbar\omega_3 + \ell(\ell + 1)\hbar B.$$

2.2 Recall without calculation the parity of the eigenfunctions of the one-dimensional harmonic oscillator, then deduce the action of the operator exchanging the two oxygen nuclei on state $|n\rangle \otimes |\ell, m\rangle$.

We know that the eigenfunctions of the one-dimensional harmonic oscillator are alternately even and odd. As shown in the diagram below, exchanging the two oxygen nuclei is equivalent to changing \vec{u} to $-\vec{u}$ and then changing ζ and $-\zeta$.



We deduce

$$\hat{P}_{12}|n\rangle \otimes |\ell, m\rangle = (-1)^n |n\rangle \otimes (-1)^\ell |\ell, m\rangle = (-1)^{n+\ell} |n\rangle \otimes |\ell, m\rangle.$$

2.3 Deduce the permitted values for ℓ depending on the values taken by n .

As above, we must have $\hat{\Pi}|\psi\rangle = |\psi\rangle$ for any physically acceptable state $|\psi\rangle$. We deduce that $n + \ell$ must be even for the state to be physically acceptable. The allowed values for ℓ are therefore even numbers when n is even, and odd numbers when n is odd.

2.4 It is assumed that at room temperature the system can be randomly in one of the states $|0\rangle \otimes |\ell, m\rangle$, where ℓ satisfies the condition obtained in the previous question. Calculate the matrix element $\langle n' | \otimes \langle \ell', m' | \hat{\vec{\mu}} \cdot \vec{\mathcal{E}}_0 |0\rangle \otimes |\ell, m\rangle$, where it will be assumed that the electric field $\vec{\mathcal{E}}_0$ is aligned along the z axis, then identify the $|n'\rangle \otimes |\ell', m'\rangle$ states accessible following interaction with infrared radiation.

You will need to use the relation

$$Y_{\ell,m}(\theta) \cos \theta = \alpha_{\ell,m} Y_{\ell+1,m}(\theta) + \beta_{\ell,m} Y_{\ell-1,m}(\theta), \quad (9)$$

where $\alpha_{\ell,m}$ and $\beta_{\ell,m}$ are known real coefficients whose explicit expression as a function of ℓ and m will not be necessary. We obviously have $\beta_{\ell,\ell} = 0$.

We have $\hat{\vec{\mu}} \cdot \vec{\mathcal{E}}_0 = \mathcal{E}_0 \hat{\mu}_z = \mu_3 \mathcal{E}_0 (\hat{a}_3 + \hat{a}_3^\dagger) \hat{u}_z$, i.e.

$$\hat{\vec{\mu}} \cdot \vec{\mathcal{E}}_0 |0\rangle \otimes |\ell, m\rangle = \mu_3 \mathcal{E}_0 |1\rangle \otimes \hat{u}_z |\ell, m\rangle.$$

The matrix element we are looking for is the scalar product $\langle n|1\rangle$, which means $n = 1$. Furthermore, we obtain the matrix element

$$\begin{aligned} \langle \ell', m' | \hat{u}_z | \ell, m \rangle &= \int_0^\pi \int_0^{2\pi} Y_{\ell',m'}(\theta) \cos \theta Y_{\ell,m}(\theta) \sin \theta d\theta d\varphi \\ &= \alpha_{\ell,m} \langle \ell', m' | \ell + 1, m \rangle + \beta_{\ell,m} \langle \ell', m' | \ell - 1, m \rangle. \end{aligned}$$

As the spherical harmonics are orthogonal, we deduce that $m' = m$ and that $\ell' = \ell + 1$ or $\ell - 1$, the matrix element being $\alpha_{\ell,m}$ or $\beta_{\ell,m}$ respectively. We deduce that the only non-zero matrix elements are

$$\langle 1 | \otimes \langle \ell + 1, m | \hat{\vec{\mu}} \cdot \vec{\mathcal{E}}_0 |0\rangle \otimes |\ell, m\rangle = \mu_3 \mathcal{E}_0 \alpha_{\ell,m}$$

and

$$\langle 1 | \otimes \langle \ell - 1, m | \hat{\vec{\mu}} \cdot \vec{\mathcal{E}}_0 |0\rangle \otimes |\ell, m\rangle = \mu_3 \mathcal{E}_0 \beta_{\ell,m}.$$

2.5 Express as a function of ω_3 and B the corresponding energy differences, $E_{n',\ell'} - E_{0,\ell}$, according to the allowed values of $\Delta\ell = \ell' - \ell$.

The permitted values of $\Delta\ell$ are ± 1 . For $\Delta\ell = +1$, we obtain

$$E_{1,\ell+1} - E_{0,\ell} = \hbar\omega_3 + \hbar B ((\ell + 1)(\ell + 2) - \ell(\ell + 1)) = \hbar\omega_3 + 2(\ell + 1)\hbar B,$$

while for $\Delta\ell = -1$ (and $\ell \geq 2$), we get

$$E_{1,\ell-1} - E_{0,\ell} = \hbar\omega_3 + \hbar B ((\ell - 1)\ell - \ell(\ell + 1)) = \hbar\omega_3 - 2\ell\hbar B.$$

2.6 Using the previous results, discuss the infrared spectrum shown in Fig. 5. You can

- explain qualitatively the general shape of the absorption spectrum,
- deduce from the spectrum the numerical values of B and the length of the CO bond,
- explain the growth and decay of the spectrum envelope away from the central frequency (assuming for sake of simplicity that $\alpha_{\ell,m}$ and $\beta_{\ell,m}$ are independent of ℓ and m),
- discuss features not predicted by the simplified theoretical model developed in this exercise.

We therefore expect to observe a series of evenly-spaced lines at a frequency above (resp. below) ω_3 when $\Delta\ell = +1$ (resp. -1). The expected transition frequencies for $\Delta\ell = +1$ are $\omega_3 + 2(\ell + 1)B$ with $\ell \in \{0, 2, 4, \dots\}$, i.e. $\omega_3 + 2B$, $\omega_3 + 6B$, $\omega_3 + 10B$, and so on. Similarly, for $\Delta\ell = -1$ the expected frequencies are $\omega_3 - 2\ell B$ with $\ell \in \{2, 4, \dots\}$, i.e. $\omega_3 - 4B$, $\omega_3 - 8B$, and so on. This is exactly what we see on the figure, with lines regularly spaced by an amount equal to $4B$ (at least for the first lines on either side of the central frequency).

To determine the spacing between absorption lines, we measure 247 (resp. 223) GHz for the first 5 periods below (resp. above) ω_3 . Taking the average and dividing by 5, we deduce a spacing $4B/(2\pi)$ of around 47 GHz, i.e. $B/(2\pi) \approx 11.8$ GHz.

To determine the length r_0 of the CO link, we can write $I = 2m_O r_0^2$ and use the expression $B = \hbar/(2I) = \hbar/(4m_O r_0^2)$. We deduce

$$r_0 = \sqrt{\frac{\hbar}{4m_O B}} = \sqrt{\frac{1.05 \times 10^{-34}}{4 \times 16 \times 1.67 \times 10^{-27} \times 2\pi \times 11.8 \times 10^9}} \approx 115 \text{ pm}.$$

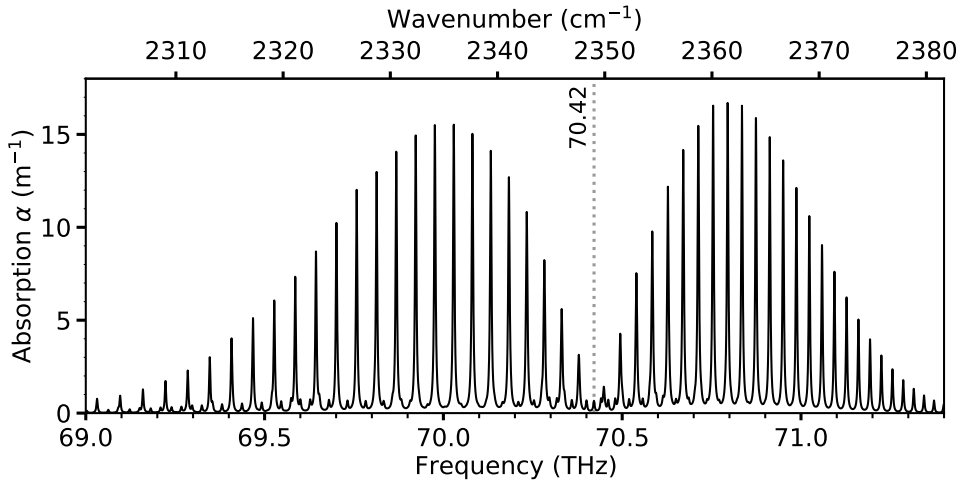


FIGURE 5 – Infrared absorption spectrum of CO_2 near the frequency ω_3 .

According to the hypothesis proposed in the statement, the transition matrix elements are all identical. The amplitude of each absorption line is then simply proportional to the number of possible initial states, i.e. the degeneracy $2\ell + 1$, or $|\alpha|^2, 5|\alpha|^2, 9|\alpha|^2, \dots$ for $\omega > \omega_3$ and $5|\beta|^2, 9|\beta|^2, \dots$ for $\omega < \omega_3$. This affine variation in line amplitude with ω is perfectly verified on the figure up to $\ell = 8$. To account for the decay of the absorption spectrum for larger values of ℓ , the Boltzmann factor $\exp(-(E_{0,\ell} - E_{0,0})/(k_B T)) = \exp(-\ell(\ell + 1)B/\omega_T)$ must be taken into account. For low values of ℓ , this factor is close to 1 : for example, for $\ell = 8$, we obtain $\exp(-8 \times 9 \times 11.5/6000) \approx 0.87$, which explains the affine variation already discussed above. For $\ell \gg 1$, we can write $\ell \approx |\omega - \omega_3|/(2B)$ and $(E_{0,\ell} - E_{0,0})/\hbar \approx \ell^2 B \approx (\omega - \omega_3)^2/(4B)$. The result is

$$\exp(-(E_{0,\ell} - E_{0,0})/(k_B T)) \approx \exp\left(-\frac{(\omega - \omega_3)^2}{4B\omega_T}\right),$$

i.e. a Gaussian distribution with standard deviation $\Delta\omega/(2\pi) = \sqrt{2B\omega_T}/(2\pi) \approx 370$ GHz. Taking into account the degeneracy factor in $2\ell + 1 \propto |\omega - \omega_3|$, we therefore expect a $|\omega - \omega_3| \exp(-(\omega - \omega_3)^2/(2\Delta\omega^2))$ distribution, which corresponds exactly to the observed function. This function is expected to peak at $|\omega - \omega_3| = \Delta\omega$, which is in excellent agreement with the observed value (measured at approximately 390 GHz instead of 370 GHz).

Finally, we can see that the absorption lines are not quite equidistant for large ℓ values, with the spacing decreasing as the frequency of the absorbed photon increases. To explain this discrepancy with our model, we can put forward the hypothesis that the rotational constant (i.e. the moment of inertia) may not be the same in the vibrational ground state as in the excited state.

3. Ro-vibrational spectrum associated with bending modes

This final section uses some of the results demonstrated in Exercise 2.

We now combine the rotational motion with the two bending modes of frequency ω_1 (this time neglecting the stretching modes). The theoretical treatment is considerably more complicated, since both rotational and bending motions contribute to the total angular momentum $\hat{\vec{L}}$ of the molecule. We assume that $\hat{\vec{L}}$ commutes with its projection $\hat{K} = \hat{\vec{L}} \cdot \hat{\vec{u}} = \hat{\vec{u}} \cdot \hat{\vec{L}}$ along the \vec{u} axis of the molecule. We also admit that this projection corresponds to the angular momentum \hat{K} already studied in exercise 2. The projection of the angular momentum in the plane perpendicular to the axis of the molecule is called $\hat{\vec{L}}_{\perp} = \hat{\vec{L}} - \hat{K}\hat{\vec{u}}$. The Hamiltonian is now written

$$\hat{H} = \hat{H}_1 + \hbar B \frac{\hat{\vec{L}}_{\perp}^2}{\hbar^2}, \quad (10)$$

where B is the rotational constant introduced above. The observables \hat{H}_1 , \hat{K} , \hat{L}^2 and \hat{L}_z commute with each other and can be diagonalized in the common eigenbasis $\{|n, k; \ell, m\rangle\}$, with the same eigenvalues as those obtained in part 1 of exercise 2 and part 1 of this exercise. However, given the more complex motion of the molecule, the corresponding wave functions are no longer proportional to the spherical harmonics $Y_{\ell,m}(\theta, \varphi)$, so the selection rules established in 2.4 are modified. We admit that infrared transitions are now possible for $\Delta\ell = -1, 0$, or $+1$.

3.1 Knowing that $\hat{L}^2 = \hat{L}_\perp^2 + \hat{K}^2$, show that $|n, k; \ell, m\rangle$ is an eigenvector of \hat{L}_\perp^2 for an eigenvalue to be determined, then deduce the expression of the energy $E_{n,k,\ell}$ associated with \hat{H} .

Knowing that $\hat{L}_\perp^2 = \hat{L}^2 - \hat{K}^2$, we can write

$$\hat{L}_\perp^2 |n; k, \ell, m\rangle = (\ell(\ell+1)\hbar^2 - (k\hbar)^2) |n; k, \ell, m\rangle = (\ell(\ell+1) - k^2)\hbar^2 |n; k, \ell, m\rangle$$

We thus obtain

$$E_{n,k,\ell,m} = (n+1)\hbar\omega_1 + (\ell(\ell+1) - k^2)\hbar B.$$

For the record, let us derive the commutation relations. Since observable \hat{u} is a vector observable, it obeys the commutation relation $[\hat{L}_i, \hat{u}_j] = i\hbar\epsilon_{ijk}\hat{u}_k$, where ϵ_{ijk} is the Levi-Civita tensor. In particular, we deduce $[\hat{u}_i, \hat{L}_j\hat{u}_j] = i\hbar\epsilon_{ijk}\hat{u}_k\hat{u}_j = 0$ (because $\hat{u} \times \hat{u} = 0$). Furthermore, $[\hat{L}_i, \hat{K}] = [\hat{L}_i, \hat{L}_j\hat{u}_j] = i\hbar\epsilon_{ijk}\hat{L}_k\hat{u}_j + \hat{L}_j i\hbar\epsilon_{ijk}\hat{u}_k = 0$ and $[\hat{K}, \hat{u}_i] = [L_j\hat{u}_j, u_i] = i\hbar\epsilon_{jik}u_k\hat{u}_j = 0$. The result is

$$\hat{L}_\perp \cdot \hat{K}\hat{u} = \hat{L} \cdot \hat{K}\hat{u} - \hat{K}\hat{u} \cdot \hat{K}\hat{u} = \hat{L} \cdot \hat{u} \hat{K} - \hat{K}^2\hat{u}^2 = 0$$

and

$$\hat{K}\hat{u} \cdot \hat{L}_\perp = \hat{K}\hat{u} \cdot \hat{L} - \hat{K}^2 = 0.$$

We finally obtain $\hat{L}^2 = (\hat{L}_\perp + \hat{K}\hat{u})^2 = \hat{L}_\perp^2 + \hat{K}^2$.

3.2 The electric field associated with the infrared radiation is assumed to be polarized along the z axis. Explain why $\hat{\mu}_z$ commutes with \hat{L}_z , then deduce that an infrared transition must respect the selection rule $\Delta m = 0$.

If the field is polarized along the z axis, the system will be invariant to rotation about the z axis. In fact, it's immediate that the observable $\hat{\mu}_z$ is invariant under the action of a rotation around the z axis, and therefore commutes with \hat{L}_z . Similar to the reasoning already carried out in Exercise 2 (question 2.4), we deduce that the matrix elements of $\hat{\mu}_z$ can only couple states with the same value of m , from which we derive the selection rule $\Delta m = 0$ so that the matrix element involved in eq. 1 is non-zero.

3.3 Consider a transition from state $|0, 0; \ell, m\rangle$ to state $|1, k; \ell + \Delta\ell, m\rangle$. Recall the possible values of k , then deduce the transition frequencies in the three cases $\Delta\ell = -1, 0$ or 1 . Based on these results, interpret the part of the spectrum shown in Fig. 3 located between 19 and 21 THz.

We saw in the previous exercise that for the level $n = 1$ of the harmonic oscillator we had $k = \pm 1$, i.e. $k^2 = 1$. From this we deduce :

For $\Delta\ell = 1$,

$$E_{1,\pm 1,\ell+1} - E_{0,0,\ell} = \hbar\omega_1 + ((\ell+1)(\ell+2) - 1 - \ell(\ell+1))\hbar B = \hbar\omega_1 + (2\ell+1)\hbar B.$$

For $\Delta\ell = 0$,

$$E_{1,\pm 1,\ell} - E_{0,0,\ell} = \hbar\omega_1 + (\ell(\ell+1) - 1 - \ell(\ell+1))\hbar B = \hbar\omega_1 - \hbar B.$$

For $\Delta\ell = -1$,

$$E_{1,\pm 1,\ell-1} - E_{0,0,\ell} = \hbar\omega_1 + ((\ell-1)\ell - 1 - \ell(\ell+1))\hbar B = \hbar\omega_1 - (2\ell+1)\hbar B.$$

Apart from a slight frequency shift, the two cases $\Delta\ell = \pm 1$ are similar to what we had obtained for the stretching mode, giving rise to the very narrow lines observed Fig. 3. There are 18 rotational lines covering a spectral width of about 860 GHz. This yields a value similar to that already obtained, $B/(2\pi) \approx 12$ GHz, in agreement with our theoretical model. However, we now observe a new transition corresponding to $\Delta\ell = 0$ close to ω_1 , independent of ℓ . This new transition is much more intense, as all rotational states absorb at the same frequency. Our model is therefore in excellent agreement with the central part of the absorption spectrum shown in Fig. 3

3.4 Using the results obtained in the previous exercise, explain the general shape of the spectrum shown in Fig. 3.

From what we've just seen, each vibrational transition will give rise to a central line ($\Delta\ell = 0$) and rotational lines on either side ($\Delta\ell = \pm 1$). The same applies to new transitions arising from Fermi resonances. The result will be transitions from the $|1; \pm 1, \ell, m\rangle$ state to the two possible linear combinations between the $|2; 0, \ell + \Delta\ell, m\rangle$ states and the $|1\rangle$ state of the symmetric stretching

mode, giving rise to the two intense transitions observed at 18.5 and 21.6 THz (for $\Delta\ell = 0$) but also to the series of narrow lines on either side (for $\Delta\ell = \pm 1$). The same phenomenon is repeated for the transition from $n = 2$ to $n = 3$, finally giving rise to the triangular-shaped spectrum (in semi-logarithmic scale) seen in Fig. 3.

- 3.5** Figure 6 represents the infrared spectrum emitted by the Earth into space (also called spectral emittance), calculated using a simplified radiative transfer model¹. The emission spectra, represented near ω_1 , are based on three models of CO₂ absorption spectra : the first (a) only considers the vibration at ω_1 , the second (b) includes molecular rotations but does not account for Fermi resonance, while the third (c) uses the spectrum shown in Figure 3, which also includes the Fermi resonance studied in Exercise 2. The additional absorbed power (called radiative forcing) due to a doubling of the CO₂ concentration according to these three models is respectively (a) 0.1, (b) 1.8, and (c) 4.1 W/m². Comment on these results using Figures 3 and 6 and then conclude.

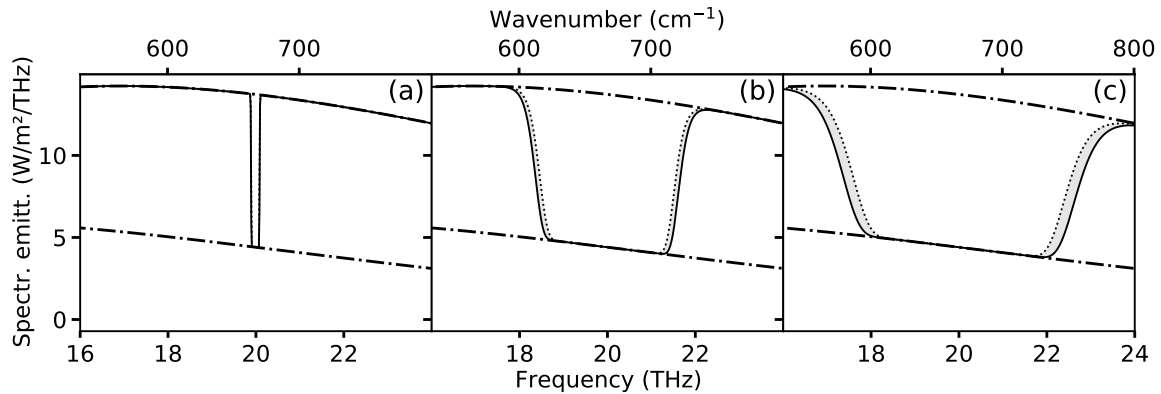


FIGURE 6 – Representation of the Earth’s spectral emittance near ω_1 for a CO₂ concentration of 280 ppm (dotted line) and 560 ppm (solid line). The theoretical model considers only the vibration at ω_1 (a), vibrations and rotations without (b) or with (c) Fermi resonance. The dashed lines represent the blackbody emission spectrum for temperatures of 288 K (upper curve) and 216 K (lower curve). The latter value corresponds to the temperature at the top of the atmosphere.

In all three cases, two regions can be distinguished on the spectra shown in Fig. 6 : away from the CO₂ absorption band, the atmosphere is transparent, so that we observe blackbody radiation emitted by the earth’s surface, at a temperature of 288 K. At the center of the absorption band, the atmosphere is totally opaque, so that the radiation emitted to space is solely the result of blackbody radiation emitted by the upper layer of the atmosphere, at a temperature of 216 K. In case (a), the absorption spectrum - consisting of the single vibrational line at ω_1 - is very narrow and the radiative forcing is extremely weak, in line with this simplistic idea of a “saturation” of the greenhouse effect. In case (b), the infrared spectrum of CO₂ (the central region of the spectrum shown in Fig. 3) is much broader, with a parabolic shape on a semi-logarithmic scale. The atmosphere is now totally opaque over a band about 3 THz wide. When the CO₂ concentration is doubled, the absorption coefficient is doubled, so that the opacity band widens slightly, giving rise to a significant increase in absorbed power. Finally, in case (c), the Fermi resonance gives rise to a considerable broadening of the CO₂ absorption spectrum, due to new transitions emanating from excited vibrational levels. The spectrum takes on the triangular shape in semi-logarithmic scale shown in Fig. 3, so that the opacity band is now much wider, covering around 5 THz. This band is also likely to widen further following a doubling of CO₂, due to the slower decay of the absorption spectrum associated with its triangular shape. As Fig. 6(c) shows, the transition from total opacity to total transparency covers a much wider spectral band, giving rise to greater radiative forcing. It is therefore the combination of molecular rotation and Fermi resonance that gives rise to CO₂’s major impact on climate.

The value obtained with this very simple model, 4.1 W/m², is remarkably close to the exact value, 3.7 W/m², obtained using much more elaborate climate models. Furthermore, the quasi-triangular shape (in semi-logarithmic scale) of the CO₂ absorption spectrum shown in Fig. 3 explains the well-known logarithmic variation of radiative forcing as a function of CO₂ concentration (for example see courses Engineering sustainability, CCH_40002, and Energy and environment, PHY_51055).

1. D. Louapre, github.com/scienceetonnante/RadiativeForcing (2023).

Multiplying the CO_2 concentration by a factor of λ shifts the absorption spectrum upwards on the semi-logarithmic graph by an amount proportional to $\log \lambda$, which - given the triangular shape of the spectrum - widens the opacity band by an amount also proportional to $\log \lambda$. The increase in energy absorbed by CO_2 is therefore proportional to the logarithm of its concentration.

For more information, you can consult the references below

- M. Joffre, *Quantum physics online* (2024).
- R. Wordworth, J.T. Seeley, K.P. Shine, *Fermi resonance and the quantum mechanical basis of global warming*, Planetary Science Journal **5**, 67 (2024), arxiv.org/abs/2401.15177.
- D. Louapre, *Saturation de l'effet de serre : le réchauffement a-t-il atteint sa limite ?*, Science étonnante (2023), www.youtube.com/watch?v=ewc8FBtEKPs.
- D. M. Romps, J.T. Seeley, J.P. Edman, *Why the forcing from carbon dioxide scales as the logarithm of its concentration*, Journal of Climate **35**, 4027 (2022).
- IPCC's sixth assessment report (AR6), *the physical science basis* (2021).
- J.L. Dufresne, V. Eymet, C. Crevoisier, J.Y. Grandpeix, *Greenhouse effect: the relative contributions of emission height and total absorption*, Journal of Climate **33**, 3827 (2020).
- D.J. Wilson, J. Gea-Banacloche, *Simple model to estimate the contribution of atmospheric CO_2 to the Earth's greenhouse effect*, Am. J. Phys. **80**, 306 (2012).
- R. Pierrehumbert, *What Ångström didn't know*, realclimate.org (2007).
- D.M. Dennison, *The infrared spectra of polyatomic molecules, part I*, Rev. Mod. Phys. **3**, 280 (1931), *The infrared spectra of polyatomic molecules, part II*, Rev. Mod. Phys. **12**, 175 (1940).
- E. Fermi, *Über den Ramaneffekt des Kohlendioxyds*, Zeit. Phys. **71**, 250 (1931).